

RESEARCH

Open Access



A highly efficient resource slicing and scheduling optimization algorithm for power heterogeneous communication networks based on hypergraph and congruence entropy

Wendi Wang^{1*}, Chengling Jiang¹, Linqing Yang¹, Hong Zhu¹ and Dongxu Zhou¹

*Correspondence:
wwdseu@163.com

¹ State Grid Jiangsu Electric Power Co., Ltd. Nanjing Power Supply Branch, Nanjing 210019, China

Abstract

New services, such as distributed photovoltaic regulation and control, pose new service requirements for communication networks in the new power system. These requirements include low latency, high reliability, and large bandwidth. Consequently, power heterogeneous communication networks face the challenge of maintaining quality of service (QoS) while enhancing network resource utilization. Therefore, this paper puts forward a highly efficient optimization algorithm for resource slicing and scheduling in power heterogeneous communication networks. Our first step involves establishing an architectural description model of heterogeneous wireless networks for electric power based on hypergraph. This model characterizes complex dynamic relationships among service requirements, virtual networks, and physical networks. The system congruence entropy characterizes the degree of matching between the service demand and resource supply. Then an optimization problem is formed to maximize the system congruence entropy through dynamic resource allocation. To solve this problem, a joint resource allocation and routing method based on Lagrangian dual decomposition is proposed. These methods provide the optimal solutions of the nodes and link mappings of service function chains. The simulation results demonstrate that the proposed algorithm in this paper can greatly enhance resource utilization and also meet the QoS requirements of various services.

Keywords: Power system, Heterogeneous communication networks, Resource slicing, Hypergraph, Congruence entropy

1 Introduction

With the widespread integration of distributed power generation into the grid, the operational mode of power grid dispatching has shifted to coordinated control of source–grid–load–storage, multi-level coordination of microgrid transmission and distribution. This has led to the emergence of new services of new power system, including distributed photovoltaic regulation, precise load control, and distribution network protection.

These diversified new power services require various performance metrics such as network throughput, latency, connections, and reliability. Currently, communication access on the “last mile” offers multiple options, including electric power wireless private networks, 5G networks, and 4G short multiplexing private networks. The electric power wireless private network offers small particle control services such as load control, power distribution automation, distribution substation monitoring, and distributed power supply. These services provide technical advantages in ensuring safety and reliability. However, the construction of a new electric power system has created a gap in the existing electric power wireless private network technology’s communication technology indicators, including delay, bandwidth, reliability, and other aspects necessary for emerging services. Therefore, there is significant room for improvement. It is essential to integrate 5G slicing and other advanced technologies to compensate for and optimize the technical limitations of the private network. Additionally, wireless private network bearing solutions must be proposed to meet the bearing requirements of new services while safeguarding existing investments.

The advancement of 5G communication technology will undeniably facilitate the profound convergence of both the power industry and communication information technology, trigger modifications within the industrial chain, stimulate software and hardware ecological structure, and produce immense economic and social advantages. By collaborating with the private network of the grid company, the low latency, high reliability, and large bandwidth, among other characteristics of 5G networks, can significantly enhance network performance in terms of rate, delay, and security. This allows for an all-round perception of each unit of the source network, load, and storage, enabling wide-area control and regulation of the entire power system’s generation, transmission, transformation, distribution, and utilization.

In the midst of diverse service scenarios and requirements, network slicing technology has become a pivotal enabler for 5G networks due to its distinct characteristics. Network slicing can be understood as a virtualized private network that spans the entire length of a mobile communication system and is made up of a sequence of virtual network functions (VNFs). Currently, researchers from domestic and international entities have conducted extensive studies on the resource management components of network slicing. Literature [1] establishes an end-to-end delay analysis model for 5G power slicing. It carefully examines the end-to-end delay of three typical power services, introducing an innovative delay rate guarantee enhancement algorithm. In addition, it quantifies and introduces three guaranteed degree factors to address specific challenges in power services, thus ensuring efficient use of system resources. On a different note, [2] describes the advantages of hypergraph theory in modeling complex data associations and outlines the current common approaches to hypergraph learning. In [3], the authors introduce a hypergraph clustering model that aligns with the compatibility relationship among various VNF instance performances, forming a mathematical framework for resource management in network slicing. To achieve the optimal resource allocation. Literature [4] introduces hypergraph theory to deal with sliced links and connections and proposes a new hypergraph-based network slicing framework exploiting the generalization property of hypergraphs to provide faster processing speed and better resource allocation. [5] Transforms the problem of interference reduction in NOMA into a maximum weighted

clique set problem in hypergraph theory, obtaining higher spectral efficiency and system performance. In [6], the authors utilize the hypergraph model to effectively solve the resource allocation problem in heterogeneous ultra-dense networks and significantly improve the spectral efficiency of cellular networks. [7] developed a mixed integer linear programming model for 5G network slicing. The model prioritizes slicing node factors, including topological characteristics, resource utilization, and delay time, using the VIKOR method. To configure the slicing links, the model employs the shortest path algorithm for determining the physical paths. Addressing the issue of spectrum sharing in cognitive capacity harvesting networks, the authors in [8] propose a strategy for sharing spectrum among network slices. This approach, which utilizes the 4D conflict graph model and the opportunity capacity model, optimizes the use of available spectrum resources, ultimately improving channel utilization.

Literature [9] innovatively suggests a genetic algorithm to resolve the resource allocation challenge in network slicing. This algorithm, guided by intelligent assessments of virtual network node resource demands, achieves a global optimal solution. Notably, it reduces underlying network overhead, enhances underlying network revenue, and improves the success of virtual network mapping compared to algorithms based on greedy strategies. Furthermore, [10] introduces a metric for VNF reliability requirements by considering the resource requirements and location constraints of VNFs. Building upon this, a sliced reliable mapping model is established, aiming to maximize gains from reliable VNF deployment while minimizing link bandwidth resource overhead. In the context of power services, the authors in [11] define the power service levels based on the QoS requirements of various types of power services. They propose a dynamic resource allocation strategy for hierarchical network slicing, utilizing a utility maximization algorithm. This strategy conducts two resource allocations for the slicing layer and the user layer, ensuring fairness while guaranteeing the quality of the user's experience. To address data security concerns in the current information collection scenario, [12] introduces a distributed multi-node slicing model based on blockchain. This model is designed to analyze examples and applications for tackling issues like theft, tampering, and destruction during data transmission and storage in the electric power information collection service. Recognizing the current lack of end-to-end global delay optimization methods for electric power services, [13] proposes a 5G network slicing resource scheduling and mapping method tailored to the characteristics of electric power services. This method prioritizes three key aspects: slices, virtual network functions, and physical resources. It meticulously filters and prunes each candidate matching pair, iteratively solving the optimization problem.

However, the development of the new power system has led to increasingly diverse service demands and a greater variety of network elements. This has resulted in an unprecedented scale of services, network nodes, and complex relationships within and between them. Current researches lack a mathematical method to describe the complex dynamic relationship between multiple services, networks, and slices, as well as assessment indexes for the overall advantages and disadvantages of the network architecture. Thus, this makes it difficult to accurately identify the factors affecting network performance and provide mathematical analytical solutions. Additionally, some of the existing literatures only address the requirements of a single business scenario, without

considering the actual application of multi-service scenarios. Furthermore, some of the literatures on virtual network functions only take into account a single resource situation, without considering the optimization of multi-dimensional resource constraints. Therefore, when facing the new dynamic demands of power systems on communication networks, it is important to consider whether a suitable evaluation index can be found to measure the complexity or merit of the network architecture. Based on this index, the multi-dimensional network resources can be adjusted and scheduled on-demand to enhance its flexibility, maximize the value of the grid infrastructure, and serve more users.

To achieve this, our paper presents a hypergraph and congruence entropy-based methodology that dynamically optimizes resource slicing and scheduling for power heterogeneous communication networks. Firstly, we employ a hypergraph perspective to model the architecture of a power heterogeneous wireless network, which includes the physical, logical, and service domains. We abstract the core characteristics of power wireless network elements across multiple levels and dimensions, and then quantify and refine the complex relationships among these elements to create a comprehensive theoretical framework. The proposed method for dynamic resource slicing and scheduling optimization aims to meet the demands of large-capacity, low-latency, and highly reliable services within the new electric power system. This is achieved through the use of entropy-increasing matching technology, which matches service demand with available network resources. The main contributions of the proposed algorithm are as follows:

- A hypergraph-based architectural description model of heterogeneous wireless networks for electric power is established, and the vertices and hyperedges of the hypergraph between physical-logical-service domains are designed to characterize the complex dynamic relationships among service requirements, virtual networks, and physical networks.
- The system congruence entropy is defined to characterize the degree of matching between the service demand and the actual resource supply, and then a dynamic resource slicing and scheduling optimization problem for power heterogeneous wireless networks which maximizes the system congruence entropy is formed.
- For the optimization problem of congruence entropy, a joint resource allocation and routing method based on Lagrangian dual decomposition is proposed to solve the node mapping and link mapping problems of service function chains.
- Simulation results show that the proposed algorithm in this paper is able to improve the resource utilization while satisfying the QoS of different services.

2 System model

2.1 Network architecture

As shown in Fig. 1, the electric power heterogeneous wireless network consists of power wireless private network, 5G and other converged networks, which can be categorized into three-domain architectures based on their functions: physical domain, logical domain, and service domain.

Physical domain is the abstract modeling of physical equipment such as access network, bearer network, core network, etc., which provide basic resources and run

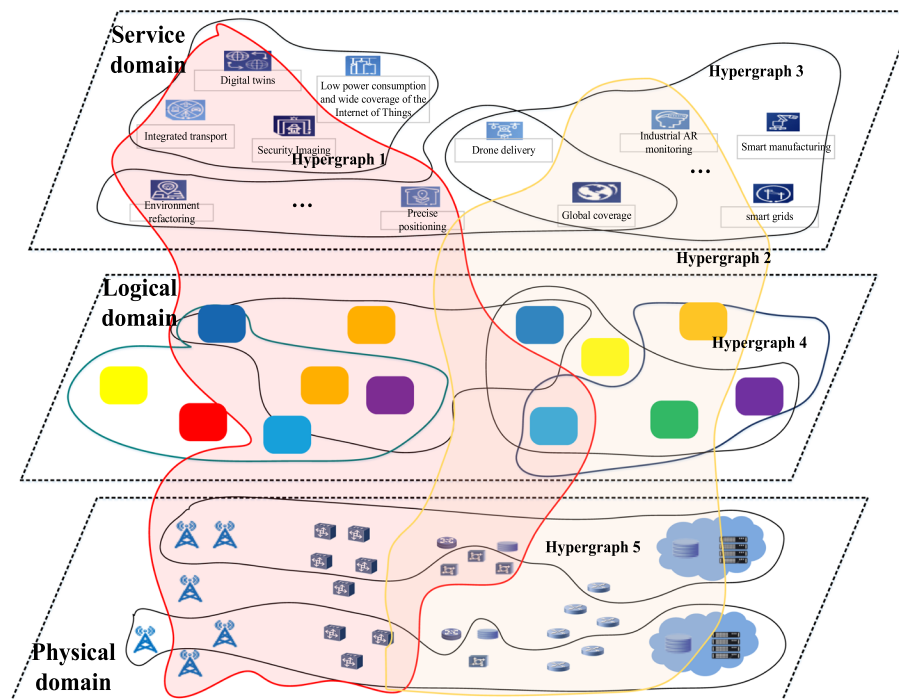


Fig. 1 Three-domain model of power heterogeneous wireless network based on hypergraph

network functions. The network components in the physical domain include base stations, routers, servers, control devices, terminals, etc., which mainly complete one or more functions of data collection, generation, storage, forwarding, reception, computation, etc., and they are the resource entities of the network. The physical domain can dynamically perceive the network state, carry out intelligent clustering and game decision-making of network components, and collaboratively schedule network resources.

In the logical realm, network services bring service requirements to fruition. The entity responsible for network service fulfillment is the service function chain (SFC). A logical sequence of virtual network function (VNF) combinations materializes the SFC, and different combinations of NFs assemble distinct network slices and private networks. Multiple closely interacting microservices are aggregated into network functions (NFs), which ultimately achieve various services, including data transmission processing and network security, through the time-ordered interactions among several NFs. Each node in the network has its own exclusive physical resources, such as computing, storage, and networking resources. Multiple virtual network functions (VNFs) can be assigned to each node. When deploying virtual network functions, it is crucial to allocate the necessary resources to VNFs upon instantiation on nodes and consider the end-to-end performance requirements of the service function chain within which they are located.

Service domain mainly categorizes the electric power service and models the various service abstractions generated by diverse scenarios. According to the communication performance requirements of electric power service, it can be divided into three categories: control class, information collection class, and mobile application class. The grid control class service imposes demanding communication delay constraints, necessitating a communication system that delivers low latency and high levels of reliability,

as well as precise power distribution automation and load control. Conversely, the acquisition class service lacks stipulations regarding latency and bandwidth, and is characterized by operations such as acquiring power consumption data and monitoring transmission lines. Intelligent inspection and mobile operation are common types of mobile applications that require significant bandwidth and network mobility. Objective evaluation of such services is important for assessing their effectiveness and improving their functionality.

2.2 Hypergraph-based three-domain characterization model for power heterogeneous networks

2.2.1 Three-domain hypergraph model

With the development of new power systems, the increasingly diverse service requirements and network elements have led to unprecedented service scale, network node scale, and various complex relationships within the network and between network nodes and services. As a generalized graph, a hyperedge can connect any number of vertices, which can capture and represent the higher-order interactions of the elements in the network and the higher-order group relationships of the network. Hyperedges surpass the description of simple edges for pairwise relations, constituting the fundamental distinction between hypergraphs and conventional graph models. Thus, the hypergraph theory is suitably tailored to effectively characterize intricate and diverse complex power networks founded on hypergraph theory principles, remarkably fitting the unique attributes of power complex heterogeneous networks.

As shown in Fig. 1, this paper establishes a three-domain characterization model for power heterogeneous wireless networks based on hypergraphs, and designs the vertices and hyperedges constituting the inter-domain hypergraphs by analyzing multiple elements of the network architecture, extracting features such as service attributes, network functional attributes, and device performance and location attributes, as well as the relationships among the attributes. The specific elements constituting the hypergraph are expressed as follows: (1) Classify and quantify services within the service domain based on varying spatiotemporal characteristics, application scenarios, and QoS requirements. (2) Determine the quantity and types of microservices within the logical domain to enable function realization at varying levels of granularity. (3) Classify and quantify network components based on type, attribute, and behavior within the physical domain. (4) Explore various combinations of service types, virtualized network functions (VNFs), and specific network components across the three domains. The hypergraph shows the various combinations of service types, VNFs, and network components, along with a mathematical description for each element in the service, logical, and physical domains. Subject-specific terms are used where necessary to enhance precision of meaning. Grammatical and spelling errors are avoided.

2.2.2 Service domain hypergraph model

In the service domain, the service is categorized into typical electric power service such as control, information collection and mobile application. Assuming that Q^u , Q^e , Q^m denote the set of typical service types in the service domain, the service domain hypergraph is modeled as $\mathcal{H}_{intra}^1(\mathcal{V}_{intra}^1, \mathbb{E}_{intra}^1)$. Each service $E_j^i, i \in (u, e, m), j \in (A, K, C)$ is a

node in the hypergraph of the service domain, and the set of nodes of the service domain $\mathcal{V}_{intra}^1 = Q$. Categorized according to the control category, the information collection category and the mobile application category and other typical electric power services, etc., the services belonging to the same category ξ^i can constitute a hyperedge within the service domain, and considering each category of service class as a hyperedge, and the service domain hyperedge set can be expressed as $\mathbb{E}_{intra}^1 = \{\xi_u, \xi_e, \xi_m\}$.

2.2.3 Logical domain hypergraph model

The set of all the service function chains that need to be mapped at the service function chain layer is $S = \{S^u, S^e, S^m\}$, S^u, S^e, S^m represent the requirements of the service function chain of each of the three categories.

The control class service function chain is represented as $S^u = \{S_a^u | a = 1, 2, \dots, A\}$ where $S_a^u = \{f_{a,1}^u, f_{a,2}^u, \dots, f_{a,|S_a^u|}^u\}$, $|S_a^u|$ denotes the length of the a^{th} service function chain of the control class, and $f_{a,n}^u$ denotes the n^{th} VNF instance in the a^{th} service function chain. For a low-latency service function chain S_a^u , the transmission delay is bounded by τ_a^u .

The functional chain of mobile application services is represented as $S^e = \{S_k^e | k = 1, 2, \dots, K\}$ where $S_k^e = \{f_{k,1}^e, f_{k,2}^e, \dots, f_{k,|S_k^e|}^e\}$, $|S_k^e|$ denoted by the functional chain of the mobile application services at the first length of the k th service function chain, $f_{k,n}^e$ denotes the n^{th} VNF instance in the k^{th} service function chain. The VNFs in the service function chain of the mobile application are allowed to deflate the traffic in order to realize the high rate transmission, and the deflation ratio of its traffic defined as $u_{f_{k,n}^e} = \frac{r_o}{r_n}$ is denoted as the data rate flowing out of the VNF and r_n is denoted as the data rate flowing into $f_{k,n}^e$ data rate of the VNF. The final rate requirement of $f_{k,n}^e$ for each such service function chain is $VR_{S_k^e}$.

The collection class service function chain is represented as $S^m = \{S_c^m | c = 1, 2, \dots, C\}$, where $S_c^m = \{f_{c,1}^m, f_{c,2}^m, \dots, f_{c,|S_c^m|}^m\}$, $|S_c^m|$ denotes the first c^{th} service function chain of the collection class of service function chains length, and $f_{c,n}^m$ denotes the n^{th} VNF instance in the c^{th} service function chain.

The virtual link between two neighboring VNFs of each service function chain is denoted as $sv_{f_{y,n}^x, f_{y,n+1}^x}$, and the initial data rate of each SFC is set to be respectively $r_{S_a^u}, r_{S_k^e}, r_{S_c^m}$. The latency of physical node i in the set of three types of hardware nodes to process the VNF is $t_{N_i^u}^{f_{a,n}^u}, t_{N_i^e}^{f_{a,n}^u}, t_{N_i^e}^{f_{k,n}^e}, t_{N_i^m}^{f_{a,n}^u}$.

The logical domain hypergraph is modeled as $\mathcal{H}_{intra}^2(\mathcal{V}_{intra}^2, \mathbb{E}_{intra}^2)$, and each service function chain vnf_g constitutes a node in the logical domain hypergraph $\mathcal{V}_{intra}^2 = S$. Each virtual network function constitutes an intra-logical domain hyperedge, and thus, the set of logical domain hyperedges is $\mathbb{E}_{intra}^2 = \{S^u, S^e, S^m\}$.

2.2.4 Physical domain hypergraph model

The communication network of the underlying physical nodes is represented by the graph $G = (N, E)$, and N denotes the set of available physical nodes at the bottom, and the set of physical nodes at the bottom, N is clustered into the three categories of general-purpose power service-specific hardware. The set of nodes N^u, N^e, N^m , $N = N^u \cup N^e \cup N^m$, the dedicated hardware nodes that perform the clustering

completion can provide better physical resources and QoS for the VNFs. When service function chain mapping is performed, the service function chains in the corresponding scenarios are preferentially mapped to the set of corresponding hardware nodes. $N_i^u, N_j^u \in N^u$ denotes the physical node i, j which is the physical device in the set N^u . The physical link between N_i^u and N_j^u is denoted as $e_{ij}^u \in e^u$, where e^u denotes the set of links of N^u physical nodes. In the physical network graph G , E denotes the set of links, where $E = e^u \cup e^m \cup e^e$. N^u, N^e, N^m are the number of physical nodes of the three types of physical nodes $|N^u|, |N^e|, |N^m|$ respectively. The transmission delay of the physical link between physical nodes i, j in the three types of power-specific hardware is denoted as $t_{e_{ij}^u}, t_{e_{ij}^e}, t_{e_{ij}^m}$. The bandwidth of the link is denoted as $B_{e_{ij}^u}, B_{e_{ij}^e}, B_{e_{ij}^m}$. The maximum utilization of resources on each link is β . The set of resources on a physical node is $Z = \{z_r | r = 1, 2, \dots, R\}$, and z_r denotes the class of resources (computing, storage, communication, etc.). The total amount of pre-deployment of all types of resources at physical node N^i for the corresponding service can be considered as $C_{N_i^u}^{z_r}, C_{N_i^e}^{z_r}, C_{N_i^m}^{z_r}$.

Assume that the set of physical domain network slices is denoted by NS^x , which is defined as

$$NS^g = \{ns_1^g, ns_2^g, \dots, ns_L^g\} \quad (1)$$

where $ns_l^g = \{N_{l1}^g, N_{l2}^g, \dots, N_{lQ}^g\}$ denotes the physical domain l_Q of physical components forming a certain slice $ns_l^g, 1 \leq l_Q \leq |N^g|$.

The physical domain hypergraph is modeled as $\mathcal{H}_{intra}^3(\mathcal{V}_{intra}^3, \mathbb{E}_{intra}^3)$, and multiple components in the physical domain enable physical domain-specific network slices, and these slices form physical domain nodes, then $\mathcal{V}_{intra}^3 = NS$, where $|NS|$ denotes the number of nodes in the physical domain. The set of network slices serving each type of service constitutes an intra-domain hyperedge; thus, the set of physical domain hyperedges is $\mathbb{E}_{intra}^3 = \{NS^u, NS^e, NS^m\}$.

2.2.5 Cross-domain hypergraph construction

In reality, the three domains are not completely independent, but rather exhibit a certain degree of correlation. For instance, there is a correlation between the services in the service domain and the virtual network functions in the logical domain, as well as a correlation between the virtual private network in the logical domain and the physical private network. Therefore, it is essential to develop an inter-domain hypergraph to objectively depict the complex and multiple connections among the components in the three domains. An inter-domain hyperedge constitutes a complete network service, which combines services in the service domain, network functions in the logical domain, and physical paths in the physical domain. A collection of distinct network services form a set of inter-domain hyperedges, ensuring a logical and causal progression of information. Precise word choices and grammatical correctness must be maintained throughout.

The three-domain inter-domain hypergraph is modeled as $\mathcal{H}_{inter}(\mathcal{V}, \mathbb{E})$, and the realization of a single complete network service is to be achieved in three-domain collaboration, and each complete network service is regarded as a three-domain inter-domain hyperedge, and the inter-domain hyperedges include each domain within the nodes, so the k th inter-domain hyperedge \mathcal{E}_{inter}^k is denoted as $\mathcal{E}_{inter}^k = \{Q_1, Q_2, \dots, S_1, S_2, \dots, NS_1, NS_2, \dots\}$,

the three-domain inter-domain hyperedge set $\mathbb{E}_{inter} = \{\mathcal{E}_{inter}^1, \mathcal{E}_{inter}^2, \dots, \mathcal{E}_{inter}^K\}$, where K denotes the number of inter-domain hyper edges. Here the network service is defined as the actual request of the user in the network, which is mapped as a service in the service domain, a network function in the logical domain, and a physical path in the physical domain in the proposed three-domain model, respectively.

3 A dynamic resource slicing method based on congruence entropy

3.1 Congruence entropy definition

In this paper, we define the degree of demand-provision matching as the system congruence entropy. ‘‘Entropy’’ can be understood as a metric or evaluation index to quantify the degree of match between the demand for resources and the actual pre-deployment of resources in a VNF in the service function chain. The specific value of this ‘‘entropy’’ can reflect the efficiency of resource utilization and the rationality of resource allocation. The utilization of network services can be quantitatively evaluated through ‘‘entropy’’ to guide rational resource allocation, thereby enhancing the performance and efficiency of network services. A dynamic slicing optimization method for power heterogeneous wireless network resources is proposed based on analysis of the characteristics of various elements within and between domains.

The collaboration of the service, logical, and physical domains is needed to execute a web service. A cross-domain hyperedge can identify the execution which takes place at a specific time. The interconnectivity of multiple network services can create overlapping elements, leading to increased complexity and reduced stability when new services are added or removed. The statistical properties of the degree of overlap between network services can be measured using cross-domain congruence entropy.

The resource allocation optimization model can be analyzed through the relationship between logical and physical domains, and the VNF mapping relationship in the chain of service functions can be defined: the binary variable $P_{f_{y,n}^x}^{N_i^x}$ is defined.

$$P_{f_{y,n}^x}^{N_i^x} = \begin{cases} 1 & \text{If } VNF_{f_{y,n}^x} \text{ maps to node } N_i^x \\ 0 & \text{else} \end{cases} \quad \forall x \in \{u, e, m\} \tag{2}$$

$\sum_{i=1}^{|N^x|} P_{f_{y,n}^x}^{N_i^x} = 1$, Ensure that a VNF can only be mapped once on the underlying physical node.

Mapping relationships for virtual links: Define the binary variables $l_{v_{f_{y,n}^x, f_{y,n+1}^x}}^{e_{ij}^x}$, $f_{y,n}^x$ and $f_{y,n+1}^x$ denote the n th and $n + 1$ th VNF instances of the chain of S_y^x service functions, respectively, $v_{f_{y,n}^x, f_{y,n+1}^x}$ denotes the virtual link between the two VNF instances, and e_{ij}^x denotes the set r of physical links between nodes i, j .

$$l_{v_{f_{y,n}^x, f_{y,n+1}^x}}^{e_{ij}^x} = \begin{cases} 1 & \text{The virtual link } v_{f_{y,n}^x, f_{y,n+1}^x} \text{ maps onto the physical link } e_{ij}^x \\ 0 & \text{else} \end{cases} \quad \forall e_{ij}^x \in e^x, \quad \forall x \in \{u, e, m\} \tag{3}$$

Then the r type resource constraint for node i in the set of physical nodes N^x is:

$$\sum_{y=1}^{|S^x|} \sum_{n=1}^{|S_y^x|} R_{f_{y,n}^x}^{zr} P_{f_{y,n}^x}^{N_i^x} \leq C_{N_i^x}^{zr}, \quad \forall x \in \{u, e, m\}, \quad \forall y \in \{a, k, c\} \# \tag{4}$$

Bandwidth physical resource constraints on link ij :

$$\sum_{y=1}^{|S^u|} \sum_{n=1}^{|S_y^u|} r_{S_y^u} \cdot l_{j_y, n^u, y, n+1}^{e^u} \leq \beta B_{e_{ij}^u}, \quad \forall e_{ij}^u \in e^u \# \tag{5}$$

$$\sum_{y=1}^{|S^x|} \sum_{n=1}^{|S_y^x|} (\prod_{t=1}^n \mu_{f_{y,t}^e}) r_{S_y^x} \cdot l_{j_y, n^e, y, n+1}^{e^e} \leq \beta B_{e_{ij}^e}, \quad \forall e_{ij}^e \in e^e \# \tag{6}$$

Control class service function chain delay constraints:

$$\sum_{n=1}^{|S_y^u|} t_{N_i^u}^{f_{y,n}^u} \cdot P_{f_{y,n}^u}^{N_i^u} + \sum_{n=1}^{|S_y^u|-1} t_{e_{ij}^u} \cdot l_{j_y, n^u, y, n+1}^{e^u} \leq \tau_y^u, \# \tag{7}$$

$\forall e_{ij}^u \in e^u, \quad \forall y \in [1, |S^u|], \quad \forall i \in N^u$

Function chain arrival flow rate constraints for mobile application class services:

$$r_{S_y^e} \cdot \prod_{n=1}^{|S_y^e|} \mu_{f_{y,n}^e} \cdot P_{f_{y,n}^e}^{N_i^e} \geq VR_{S_y^e}, \quad \forall y \in [1, |S^u|], \quad \forall i \in N^u \# \tag{8}$$

Functional chain constraints for information-gathering classes of services:

For mobile application class service function chains require high computational resources and low congestion rates. Therefore, the deployment goal should be to minimize the bandwidth usage on the physical links. As much as possible, the bandwidth load balancing on each link should be done; in other words, the remaining bandwidth on the physical link should be maximized.

$$0 < \sum_{y=1}^{|S^m|} \sum_{n=1}^{|S_y^m|} r_{S_y^m} \cdot l_{j_y, n^m, y, n+1}^{e^m} \leq \beta B_{e_{ij}^m} \# \tag{9}$$

When targeting the control class of network services, it is assumed that the n th VNF $f_{a,n}^u$ in the chain of service functions S_a^u has a demand for resources of type r of $R_{f_{a,n}^u}^{zr}$. The total amount of pre-deployment of each type of resource at physical node N_i for the corresponding network service can be considered as $C_{N_i^u}^{zr}$.

By measuring the variability between resource deployment and resource demand in the scenarios of network slicing routing and resource allocation, the proposed optimization objective aims to maximize the congruence entropy of the entire network. This objective can be transformed into a problem of maximizing the congruence entropy for the node with the smallest congruence entropy in the network. Therefore, the congruence entropy is defined to be when the control class network service Q is realized:

$$D^u = \frac{\sum_{a=1}^{|S^u|} \sum_{n=1}^{|S_a^u|} R_{f_{a,n}^u}^{zr} P_{f_{a,n}^u}^{N_i^u}}{C_{N_i^u}^{zr}} + \frac{\sum_{a=1}^{|S^u|} \sum_{n=1}^{|S_a^u|} r_{S_a^u} \cdot l_{j_a, n^u, a, n+1}^{e^u}}{\beta B_{e_{ij}^u}} \# \tag{10}$$

Using the same approach, the congruence entropy of the network service for the mobile application class of service is denoted as:

$$D^e = \frac{\sum_{k=1}^{|s^e|} \sum_{n=1}^{|s_k^e|} R_{f_{k,n}^e}^{zr} P_{f_{k,n}^e}^{N_i^e}}}{C_{N_i^e}^{zr}} + \frac{\sum_{k=1}^{|s^e|} \sum_{n=1}^{|s_k^e|} r_{s_k^e} \cdot l_{v_{f_{k,n}^e}^e} \cdot f_{k,n+1}^e}{\beta B_{e_{ij}^e}} \# \tag{11}$$

The congruence entropy of a web service in the information collection category is denoted as:

$$D^m = \frac{\sum_{c=1}^{|s^m|} \sum_{n=1}^{|s_c^m|} R_{f_{c,n}^m}^{zr} P_{f_{c,n}^m}^{N_i^m}}}{C_{N_i^m}^{zr}} + \frac{\sum_{c=1}^{|s^m|} \sum_{n=1}^{|s_c^m|} r_{s_c^m} \cdot l_{v_{f_{c,n}^m}^m} \cdot f_{c,n+1}^m}{\beta B_{e_{ij}^m}} \# \tag{12}$$

3.2 Optimization models

For the scenario of network slicing routing and resource allocation described above, the proposed optimization objective is to assess the efficacy of the network service design and deployment within a specific spatiotemporal range. This is measured by the value of the congruence entropy, where a higher value indicates a more reasonable resource design and deployment for the network service. If the congruence entropy value is nearly 1, it suggests that the resource demand and the pre-deployment of resources are closely aligned, resulting in more efficient resource utilization and the ability of the network service to operate efficiently. On the other hand, if the congruence entropy value is significantly lower than 1 and closer to 0, it indicates that there is a poor match between resource demand and resource pre-deployment. This can result in both resource wastage and degradation of service quality.

Therefore, the dynamic slicing optimization problem of power heterogeneous network resources based on hypergraph and congruence entropy is:

$$\begin{aligned} & \max \min_{N_i^x \in N} \left(\frac{\sum_{y=1}^{|s^x|} \sum_{n=1}^{|s_y^x|} R_{f_{y,n}^x}^{zr} P_{f_{y,n}^x}^{N_i^x}}}{C_{N_i^x}^{zr}} + \frac{\sum_{y=1}^{|s^x|} \sum_{n=1}^{|s_y^x|} r_{s_y^x} \cdot l_{v_{f_{y,n}^x}^x} \cdot f_{y,n+1}^x}{\beta B_{e_{ij}^x}} \right) \quad \forall x \in \{u, m\} \\ & \max \min_{N_i^x \in N} \left(\frac{\sum_{y=1}^{|s^x|} \sum_{n=1}^{|s_y^x|} R_{f_{y,n}^x}^{zr} P_{f_{y,n}^x}^{N_i^x}}}{C_{N_i^x}^{zr}} + \frac{\sum_{y=1}^{|s^x|} \sum_{n=1}^{|s_y^x|} \left(\prod_{t=1}^n \mu_{f_{y,t}^x} \right) r_{s_y^x} \cdot l_{v_{f_{y,n}^x}^x} \cdot f_{y,n+1}^x}{\beta B_{e_{ij}^x}} \right) \quad \forall x \in \{e\} \tag{13} \end{aligned}$$

s.t.

$$\sum_{n=1}^{|N^x|} P_{f_{y,n}^x}^{N_i^x} = 1 \quad \forall x \in \{u, e, m\} \tag{14}$$

$$\sum_{y=1}^{|s^x|} \sum_{n=1}^{|s_y^x|} R_{f_{y,n}^x}^{zr} P_{f_{y,n}^x}^{N_i^x} \leq C_{N_i^x}^{zr}, \quad \forall x \in \{u, e, m\}, \quad \forall y \in \{a, k, c\} \tag{15}$$

$$\sum_{y=1}^{|S^x|} \sum_{n=1}^{|S_y^x|} r_{S_y^x} \cdot l_{f_{y,n}^x, f_{y,n+1}^x}^{e_{ij}^x} \leq \beta B_{e_{ij}^x}, \quad \forall x \in \{u, m\} \tag{16}$$

$$\sum_{y=1}^{|S^x|} \sum_{n=1}^{|S_y^x|} \left(\prod_{t=1}^n \mu_{f_{y,t}^e} \right) r_{S_y^x} \cdot l_{v_{f_{y,n}^e, f_{y,n+1}^e}}^{e_{ij}^e} \leq \beta B_{e_{ij}^e}, \quad \forall e_{ij}^e \in e^e \tag{17}$$

$$\sum_{n=1}^{|S_y^u|} t_{N_i^u}^{f_{y,n}^u} \cdot P_{f_{y,n}^u}^{N_i^u} + \sum_{n=1}^{|S_y^u|-1} t_{e_{ij}^u} \cdot l_{v_{f_{y,n}^u, f_{y,n+1}^u}}^{e_{ij}^u} \leq \tau_y^u, \quad \forall e_{ij}^u \in e^u, \quad \forall y \in [1, |S^u|], \quad \forall i \in N^u$$

$$r_{S_y^e} \cdot \prod_{n=1}^{|S_y^e|} \mu_{f_{y,n}^e} \cdot P_{f_{y,n}^e}^{N_i^e} \geq VR_{S_y^e}, \quad \forall y \in [1, |S^e|], \quad \forall i \in N^e \tag{18}$$

In the above optimization problem, (13) represents the node mapping relationship constraints, (14), (15), (16) represent the resource constraints and link bandwidth constraints of the nodes, (17) represents the delay constraints of the service function chain, and (18) represents the rate constraints of the service function chain, respectively.

The complex optimization problem of the overall network deployment above is split into the following three subservice joint optimization problems.

The subproblems for the low-latency control class of operations are:

$$\max_{N_i^u \in N^u} \left(\frac{\sum_{y=1}^{|S^u|} \sum_{n=1}^{|S_y^u|} R_{f_{y,n}^u}^{zr} P_{f_{y,n}^u}^{N_i^u}}{C_{N_i^u}^{zr}} + \frac{\sum_{y=1}^{|S^u|} \sum_{n=1}^{|S_y^u|} r_{S_y^u} \cdot l_{f_{y,n}^u, f_{y,n+1}^u}^{e_{ij}^u}}{\beta B_{e_{ij}^u}} \right)$$

s.t.

$$P_{f_{y,n}^u}^{N_i^u} \in \{0, 1\}, l_{v_{f_{y,n}^u, f_{y,n+1}^u}}^{e_{ij}^u} \in \{0, 1\} \tag{19}$$

$$\sum_{n=1}^{|S_y^u|} t_{N_i^u}^{f_{y,n}^u} \cdot P_{f_{y,n}^u}^{N_i^u} + \sum_{n=1}^{|S_y^u|-1} t_{e_{ij}^u} \cdot l_{v_{f_{y,n}^u, f_{y,n+1}^u}}^{e_{ij}^u} \leq \tau_y^u, \quad \forall e_{ij}^u \in e^u, \quad \forall y \in [1, |S^u|], \quad \forall i \in N^u \tag{20}$$

$$\sum_{y=1}^{|S^u|} \sum_{n=1}^{|S_y^u|} R_{f_{y,n}^u}^{zr} P_{f_{y,n}^u}^{N_i^u} \leq C_{N_i^u}^{zr}, \quad \forall i \in N^u \tag{21}$$

The service subproblem of the collection class is to maximize the resource utilization on the nodes and on each link so that the network can access more services:

$$\max_{N_i^m \in N^m} \left(\frac{\sum_{y=1}^{|S^m|} \sum_{n=1}^{|S_y^m|} R_{f_{y,n}^m}^{zr} P_{f_{y,n}^m}^{N_i^m}}}{C_{N_i^m}^{zr}} + \frac{\sum_{y=1}^{|S^m|} \sum_{n=1}^{|S_y^m|} r_{S_y^m} \cdot l_{v_{f_{y,n}^m}^m}^{e^m}}}{\beta B_{e_{ij}^u}} \right)$$

s.t.

$$\sum_{i=1}^{|N^m|} P_{f_{y,n}^m}^{N_i^m} = 1, l_{v_{f_{y,n}^m}^m}^{e^m} \in \{0, 1\} \quad (22)$$

$$\sum_{y=1}^{|S^m|} \sum_{n=1}^{|S_y^m|} R_{f_{y,n}^m}^{zr} P_{f_{y,n}^m}^{N_i^m} \leq C_{N_i^m}^{zr}, \quad \forall i \in N^m \quad (23)$$

$$\sum_{y=1}^{|S^m|} \sum_{n=1}^{|S_y^m|} r_{S_y^m} \cdot l_{v_{f_{y,n}^m}^m}^{e^m} \leq \beta B_{e_{ij}^m} \quad \forall e_{ij}^m \in e^m \quad (24)$$

The subproblem expression for a service in the mobile application category is:

$$\min \left(\frac{\sum_{y=1}^{|S^e|} \sum_{n=1}^{|S_y^e|} R_{f_{y,n}^e}^{zr} P_{f_{y,n}^e}^{N_i^e}}}{C_{N_i^e}^{zr}} + \frac{\sum_{y=1}^{|S^e|} \sum_{n=1}^{|S_y^e|} \left(\prod_{t=1}^n \mu_{f_{y,t}^e} \right) r_{S_y^e} \cdot l_{v_{f_{y,n}^e}^e}^{e^e}}}{\beta B_{e_{ij}^e}} \right)$$

s.t.

$$P_{f_{y,n}^e}^{N_i^e} \in \{0, 1\}, l_{v_{f_{y,n}^e}^e}^{e^e} \in \{0, 1\} \quad (25)$$

$$\sum_{y=1}^{|S^e|} \sum_{n=1}^{|S_y^e|} R_{f_{y,n}^e}^{zr} P_{f_{y,n}^e}^{N_i^e} \leq C_{N_i^e}^{zr}, \quad \forall i \in N^e \quad (26)$$

$$\sum_{y=1}^{|S^e|} \sum_{n=1}^{|S_y^e|} \left(\prod_{t=1}^n \mu_{f_{y,t}^e} \right) r_{S_y^e} \cdot l_{v_{f_{y,n}^e}^e}^{e^e} \leq \beta B_{e_{ij}^e}, \quad \forall e_{ij}^e \in e^e \quad (27)$$

$$r_{S_y^e} \cdot \prod_{n=1}^{|S_y^e|} \mu_{f_{y,n}^e} \cdot P_{f_{y,n}^e}^{N_i^e} \geq VR_{s_y^e}, \quad \forall y \in [1, |S^e|], \quad \forall i \in N^e \quad (28)$$

3.3 Solving the optimization problem

For control class low-latency services, the optimization problem is as follows:

$$\max_{N_i^u \in N^u} \left(\frac{\sum_{y=1}^{|S^u|} \sum_{n=1}^{|S_y^u|} R_{f_{y,n}^u}^{Zr} P_{f_{y,n}^u}^{N_i^u}}}{C_{N_i^u}^{Zr}} + \frac{\sum_{y=1}^{|S^u|} \sum_{n=1}^{|S_y^u|} r_{S_y^u} \cdot l_{v_{f_{y,n}^u}^{fu}}^{e_{ij}^u}}}{\beta B_{e_{ij}^u}} \right)$$

s.t.

$$P_{f_{y,n}^u}^{N_i^u} \in \{0, 1\}, l_{v_{f_{y,n}^u}^{fu}}^{e_{ij}^u} \in \{0, 1\} \tag{29}$$

$$\sum_{n=1}^{|S_y^u|} t_{N_i^u}^{f_{y,n}^u} \cdot P_{f_{y,n}^u}^{N_i^u} + \sum_{n=1}^{|S_y^u|-1} t_{e_{ij}^u} \cdot l_{v_{f_{y,n}^u}^{fu}}^{e_{ij}^u} \leq \tau_y^u, \quad \forall e_{ij}^u \in e^u, \quad \forall y \in [1, |S^u|], \quad \forall i \in N^u \tag{30}$$

$$\sum_{y=1}^{|S^u|} \sum_{n=1}^{|S_y^u|} R_{f_{y,n}^u}^{Zr} P_{f_{y,n}^u}^{N_i^u} \leq C_{N_i^u}^{Zr}, \quad \forall i \in N^u \tag{31}$$

$$\sum_{y=1}^{|S^u|} \sum_{n=1}^{|S_y^u|} r_{S_y^u} \cdot l_{v_{f_{y,n}^u}^{fu}}^{e_{ij}^u} \leq \beta B_{e_{ij}^u}, \quad \forall e_{ij}^u \in e^u \tag{32}$$

Due to $P_{f_{y,n}^u}^{N_i^u}, P_{f_{y,n+1}^u}^{N_j^u} \in \{0, 1\}, l_{v_{f_{y,n}^u}^{fu}}^{e_{ij}^u} \in \{0, 1\}$ binary variable exists so the objective function is a nonconvex and the feasible set is also a nonconvex problem, so the optimization problem is a nonlinear integer programming problem. Since $l_{v_{f_{y,n}^u}^{fu}}^{e_{ij}^u}$ is the product of the node mapping relation $P_{f_{y,n}^u}^{N_i^u}, P_{f_{y,n+1}^u}^{N_j^u}$, in performing the problem solving without first considering the link mapping as the node mapping relation's product, as an independent variable to which additional constraints need to be added during problem transformation:

$$l_{v_{f_{y,n}^u}^{fu}}^{e_{ij}^u} \leq P_{f_{y,n}^u}^{N_i^u}, P_{f_{y,n}^u}^{N_i^u} + P_{f_{y,n+1}^u}^{N_j^u} - l_{v_{f_{y,n}^u}^{fu}}^{e_{ij}^u} \leq 1 \quad \forall y, n \tag{33}$$

Thus, the Lagrangian function can be expressed as:

$$\begin{aligned}
 L(p, l, \omega, \mu, \nu) = & \frac{\sum_{y=1}^{|S^u|} \sum_{n=1}^{|S_y^u|} R_{f_{y,n}^{zu}}^{zr} P_{f_{y,n}^{zu}}^{N_i^u}}{C_{N_i^u}^{zr}} + \frac{\sum_{y=1}^{|S^u|} \sum_{n=1}^{|S_y^u|} r_{S_y^u} \cdot l_{v_{f_{y,n}^{zu}}, f_{y,n+1}^{zu}}^{e_{ij}^u}}{\beta B_{e_{ij}^u}} \\
 & + \sum_{y=1}^{|S^u|} \omega_y \left(\sum_{n=1}^{|S_y^u|} t_{N_i^u}^{f_{y,n}^{zu}} \cdot P_{f_{y,n}^{zu}}^{N_i^u} + \sum_{n=1}^{|S_y^u|-1} t_{e_{ij}^u} \cdot l_{v_{f_{y,n}^{zu}}, f_{y,n+1}^{zu}}^{e_{ij}^u} - \tau_y^u \right) \\
 & + \sum_{y=1}^{|S^u|} \sum_{n=1}^{|S_y^u|} \mu_{y,n} \left(l_{v_{f_{y,n}^{zu}}, f_{y,n+1}^{zu}}^{e_{ij}^u} - P_{f_{y,n}^{zu}}^{N_i^u} \right) \\
 & + \sum_{y=1}^{|S^u|} \sum_{n=1}^{|S_y^u|} \nu_{y,n} \left(P_{f_{y,n}^{zu}}^{N_i^u} + P_{f_{y,n+1}^{zu}}^{N_j^u} - l_{v_{f_{y,n}^{zu}}, f_{y,n+1}^{zu}}^{e_{ij}^u} - 1 \right)
 \end{aligned} \tag{34}$$

The dyadic problem of the original problem is expressed as follows:

$$\min_{\omega, \nu, \mu} \max_{p, l} L(p, l, \omega, \mu, \nu)$$

s.t.

$$\sum_{y=1}^{|S^u|} \sum_{n=1}^{|S_y^u|} R_{f_{y,n}^{zu}}^{zr} P_{f_{y,n}^{zu}}^{N_i^u} \leq C_{N_i^u}^{zr}, \quad \forall i \in N^u \tag{35}$$

$$\omega_y, \mu_{y,n}, \nu_{y,n} \geq 0, \quad \forall y, n \tag{36}$$

$$\sum_{y=1}^{|S^u|} \sum_{n=1}^{|S_y^u|} R_{f_{y,n+1}^{zu}}^{zr} P_{f_{y,n+1}^{zu}}^{N_j^u} \leq C_{N_j^u}^{zr}, \quad \forall j \in N^u \tag{37}$$

$$\sum_{y=1}^{|S^u|} \sum_{n=1}^{|S_y^u|} r_{S_y^u} \cdot l_{v_{f_{y,n}^{zu}}, f_{y,n+1}^{zu}}^{e_{ij}^u} \leq \beta B_{e_{ij}^u} \quad \forall e_{ij}^u \in e^u \tag{38}$$

$$P_{f_{y,n}^{zu}}^{N_i^u} \in \{0, 1\}, \quad l_{v_{f_{y,n}^{zu}}, f_{y,n+1}^{zu}}^{e_{ij}^u} \in \{0, 1\}, \quad P_{f_{y,n+1}^{zu}}^{N_j^u} \in \{0, 1\} \tag{39}$$

where p, l denote the mapping of virtual functions and the mapping relationship of links are primitive variables, respectively, and μ, ν, ω are called dyadic variables. If the dyadic variables μ, ν, ω are known, the Lagrangian function can be rewritten as the sum of the functions of nodes and links:

$$L(p, l, \omega, \mu, \nu) = g(p) + g(l)$$

$$g(p) = \frac{\sum_{y=1}^{|S^u|} \sum_{n=1}^{|S_y^u|} R_{f_{y,n}^u}^{zr} P_{f_{y,n}^u}^{N_i^u}}}{C_{N_i^u}^{zr}} + \sum_{y=1}^{|S^u|} \omega_y \left(\sum_{n=1}^{|S_y^u|} t_{N_i^u}^{f_{y,n}^u} \cdot P_{f_{y,n}^u}^{N_i^u} \right) \tag{40}$$

$$- \sum_{y=1}^{|S^u|} \sum_{n=1}^{|S_y^u|} \mu_{y,n} P_{f_{y,n}^u}^{N_i^u} + \sum_{y=1}^{|S^u|} \sum_{n=1}^{|S_y^u|} \nu_{y,n} P_{f_{y,n}^u}^{N_i^u}$$

$$(p) = \frac{\sum_{y=1}^{|S^u|} \sum_{n=1}^{|S_y^u|} r_{S_y^u} \cdot l_{v_{f_{y,n}^u, f_{y,n+1}^u}}^{e_{ij}^u}}{\beta B_{e_{ij}^u}} + \sum_{y=1}^{|S^u|} \omega_y \left(\sum_{n=1}^{|S_y^u|-1} t_{e_{ij}^u} \cdot l_{v_{f_{y,n}^u, f_{y,n+1}^u}}^{e_{ij}^u} \right) \tag{41}$$

$$+ \sum_{y=1}^{|S^u|} \sum_{n=1}^{|S_y^u|} \mu_{y,n} l_{v_{f_{y,n}^u, f_{y,n+1}^u}}^{e_{ij}^u} + \sum_{y=1}^{|S^u|} \sum_{n=1}^{|S_y^u|} \nu_{y,n} \left(P_{f_{y,n+1}^u}^{N_j} - l_{v_{f_{y,n}^u, f_{y,n+1}^u}}^{e_{ij}^u} \right)$$

The above dyadic problem can be decomposed into two subproblems of mapping the current node of the virtual function and mapping the link relationship from the current node to the next hop for solving them separately.

$$P1 : \max_{P_{f_{y,n}^u}^{N_i^u}} g(p)$$

s.t.

$$\sum_{y=1}^{|S^u|} \sum_{n=1}^{|S_y^u|} R_{f_{y,n}^u}^{zr} P_{f_{y,n}^u}^{N_i^u} \leq C_{N_i^u}^{zr}, \quad \forall i \in N^u \tag{42}$$

$$\omega_y, \mu_{y,n}, \nu_{y,n} \geq 0, \quad \forall y, n \tag{43}$$

$$P_{f_{y,n}^u}^{N_i^u} \in \{0, 1\} \tag{44}$$

$$P2 : \max_{l_{v_{f_{y,n}^u, f_{y,n+1}^u}}^{e_{ij}^u}} g(l)$$

s.t.

$$\sum_{y=1}^{|S^u|} \sum_{n=1}^{|S_y^u|} R_{f_{y,n}^u}^{zr} P_{f_{y,n+1}^u}^{N_j} \leq C_{N_j}^{zr}, \quad \forall j \in N^u \tag{45}$$

$$\sum_{y=1}^{|S^u|} \sum_{n=1}^{|S_y^u|} r_{S_y^u} \cdot l_{v_{f_{y,n}^u, f_{y,n+1}^u}}^{e_{ij}^u} \leq \beta B_{e_{ij}^u} \quad \forall e_{ij}^u \in e^u \tag{46}$$

$$l_{v_{j_y, n}^{f_y, n+1}}^{e_{ij}^u} \in \{0, 1\}, P_{f_{j_y, n+1}}^{N_j^u} \in \{0, 1\} \quad (47)$$

$$\omega_y, \mu_{y,n}, v_{y,n} \geq 0, \quad \forall y, n \quad (48)$$

In problem $P1$, which contains the mapping relationship variable $P_{f_{j_y, n}}^{N_j^u}$ of VNFs on the underlying physical nodes, it is a traditional assignment problem, which can be carried out by the Hungarian algorithm for the mapping relation of service functions, by solving the mapping result of the current node of the $P2$ problem, which is brought to the $P1$ problem, and the mapping relation of the link $l_{v_{j_y, n}^{f_y, n+1}}^{e_{ij}^u}$ into a solution of the node mapping for the next hop to achieve link mapping problem solving. The solutions of the primal variables that can be obtained by solving the above two subproblems by iterating m times are $(P_{f_{j_y, n}}^{N_j^u})^m$ and $(l_{v_{j_y, n}^{f_y, n+1}}^{e_{ij}^u})^m$ follows the dyadic variables through the subgradient method. The formula for the $m + 1^{th}$ update of the dyadic variable is as follows:

$$\begin{aligned} \omega_y(m+1) = \omega_y(m) + \Delta(m) & \left(\sum_{n=1}^{|S_y^u|} t_{N_i^u}^{f_y, n} \cdot (P_{f_{j_y, n}}^{N_j^u})^m \right. \\ & \left. + \sum_{n=1}^{|S_y^u|-1} t_{e_{ij}^u} \cdot (l_{v_{j_y, n}^{f_y, n+1}}^{e_{ij}^u})^m - \tau_y^u \right) \end{aligned} \quad (49)$$

$$\mu_{y,n}(m+1) = \mu_{y,n}(m) + \Delta(m) \left(\sum_{y=1}^{|s^u|} \sum_{n=1}^{|s_y^u|} (l_{v_{j_y, n}^{f_y, n+1}}^{e_{ij}^u})^m - (P_{f_{j_y, n}}^{N_j^u})^m \right) \quad (50)$$

$$\begin{aligned} v_{y,n}(m+1) = v_{y,n}(m) \\ + \Delta(m) \left(\sum_{y=1}^{|s^u|} \sum_{n=1}^{|s_y^u|} \left((P_{f_{j_y, n}}^{N_j^u})^m + (P_{f_{j_y, n+1}}^{N_j^u})^m - (l_{v_{j_y, n}^{f_y, n+1}}^{e_{ij}^u})^m - 1 \right) \right) \end{aligned} \quad (51)$$

where $\Delta(m)$ denotes the step size of the dyadic variable iteration, and the product following the step size is the expression for the subgradient of the dyadic variable in the Lagrangian function, respectively.

3.4 Complexity analysis

The execution of the service function chain deployment algorithm based on pairwise decomposition proposed in this paper is a cyclic iterative process, and the number of iterations required to obtain the optimal solution is determined by the actual scenario. In each iteration, the algorithm first calculates the current node mapping results of the L VNFs and determines the mapping relationship of the links, and records the mapping location of the optimal service function chain. For the L VNFs, the pairwise variables are

updated according to Eqs. (49), (50), and (51). Therefore, the computational complexity of each iteration of each VNF is $6L$, and we assume that the maximum number of iterations is max_ite and the maximum number of service requests is M , respectively, and the subgradient function is computed a total of $6 \cdot M \cdot L \cdot max_ite$ times. Then the complexity of this algorithm is $O(M \cdot L \cdot max_ite)$.

4 Simulation design and result analysis

4.1 Simulation parameter setting

In order to evaluate the performance of the algorithm proposed in this paper, simulation experiments of the proposed algorithm program are conducted in this thesis using MATLAB 2020a software, which runs on a Windows 10 system PC with Intel-Corei7-9500, 1.80GHz CPU, and 8GB of operating memory. The proposed method in this paper is compared with the CoordVNF [14] and a simulated annealing SA based method. In CoordVNF, the authors provide a heuristic to coordinate the composition of VNF function chains in network slices as well as to map service function chains to subnet networks. We will compare the algorithm proposed in the paper with the above two algorithms in terms of service function chain request acceptance rate, load balancing degree, average execution time. In the simulation diagrams, the legend of the algorithm proposed in this paper is labeled using DD.

In the simulation process, the experimental topology adopts a physical network of 20 nodes, each node has physical resources for computing and storage, the total amount of resources in each physical node obeys a uniform distribution with a mean of 100 units and a variance of 30, the link bandwidth is 200 units, and the link delay is set to obey a uniform distribution with a mean of 3ms and a variance of 1ms. The number of service function chains to be deployed is 10–150, and there are 10 types of virtual network functions. In the initialization of service function chains, each service function chain consists of 2–4 types of virtual network functions, and the resource demand for the three types is 0.2–1 unit, and the rate demand for the transmission of service function chains is 1–5 units.

4.2 Experimental results

Figure 2 illustrates the relationship between service request numbers and success rates for acceptance of service. The experimental results indicate that acceptance success rates remain relatively stable when service requests are under 400. However, when service requests exceed 500, the acceptance success rate of the requested service function chain experiences a severe decline according to the experimental graphs. The acceptance rate for service requests with the pairwise decomposition algorithm is approximately 3% higher than that of the CoordVNF algorithm on average and about 11% higher than the SA algorithm. This disparity is primarily due to the pairwise algorithm's deployment of the service function chain, aimed at maximizing the congruence entropy, to fully utilize the physical resources of nodes and links. As a result, the algorithm can accommodate more service function chain deployments with the same resource setup, leading to better performance.

Figure 3 shows the variation in the congruence entropy of node and link bandwidth resource deployment due to different numbers of service chain requests. It is evident

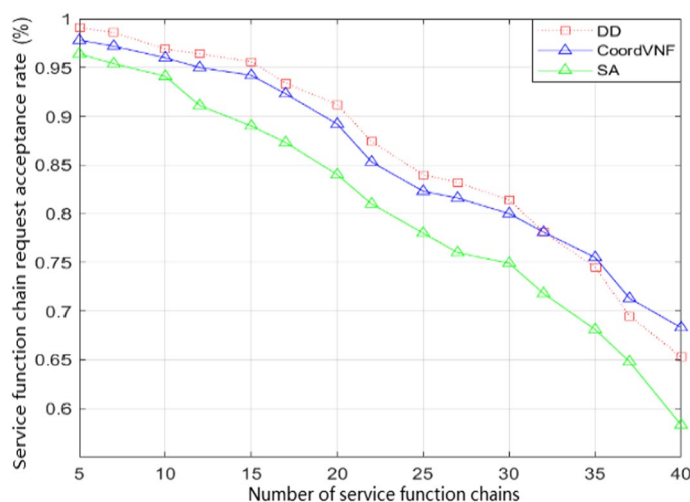


Fig. 2 Acceptance rate by number of service requests

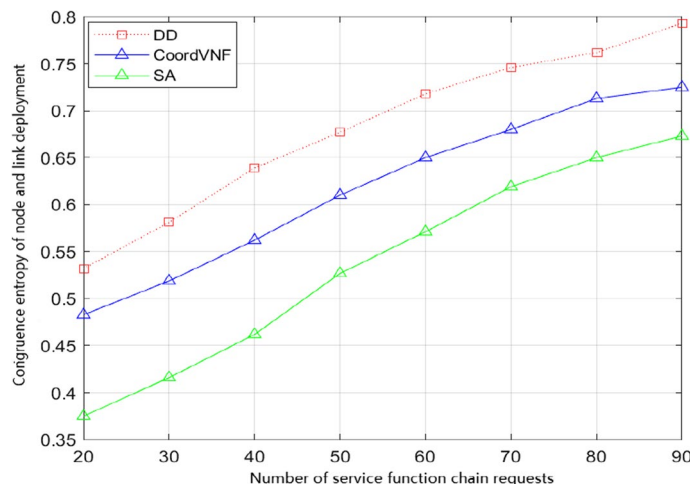


Fig. 3 The congruence entropy of node and link deployment with different service request numbers

that the congruence entropy of resource and link deployment of the physical nodes generally increases with an increase in service function chains. The table shows that the algorithm, which is based on dyadic decomposition and divides the underlying physical network into three virtual subnets based on function, improves the rationality of physical node and link bandwidth deployment by maximizing congruence entropy. This algorithm performs significantly better than CoordVNF and simulated annealing algorithms.

Figure 4 represents the average execution time required to deploy a chain of service functions with the same length as well as the same data rate at different sizes of underlying physical nodes. In order to evaluate the average execution time, we first cluster the devices with the same physical function using hypergraphs, respectively, so that the scope of the solution and the execution time can be narrowed down when performing the service function mapping. We compare the DD algorithm proposed in this paper with the CoordVNF algorithm and the SA-based approach to deploy the same service

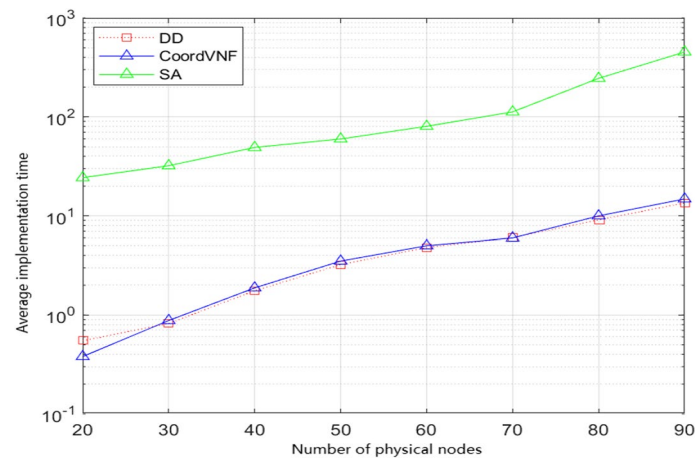


Fig. 4 Average execution time of the deployment service function chain

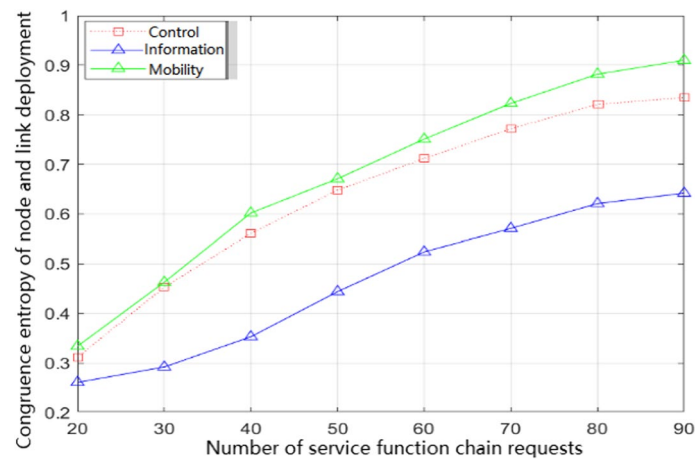


Fig. 5 Congruence entropy of different subnet-to-node and link deployments

function chain simultaneously, and the trend in the figure shows that the average execution time of our algorithm and the CoordVNF algorithm and the SA-based approach increases as the length of the service function chain increases. The execution time of the algorithm proposed in this paper is roughly similar to that of CoordVNF and is significantly shorter than that of the SA-based approach.

Since the service function chain is partitioned into three virtual subnets based on the group of physical nodes before mapping, Fig. 5 simulates the congruence entropy of node resources and link deployment for various service function chain types mapped on different subnets. The experimental topology utilized in the lower layer comprises 15 nodes and 30 links. The figure demonstrates a general trend of increased average resource use for nodes and links across the three service types as the number of service function chains grows larger. The control type service function chain consistently uses fewer physical nodes and links. Therefore, the congruence entropy of the deployment of physical nodes and links is the highest. Information type service function chains should select more physical nodes and minimize link bandwidth to reduce conflicts in

the underlying network, resulting in the lowest congruence entropy for physical node and link deployment. Since the mobile-type service function chain only considers the total delay, its performance falls between those of other chains.

5 Conclusion

This paper investigates a dynamic optimization method for slicing wireless network resources that are power heterogeneous. The approach is based on hypergraph and congruence entropy. Based on the proposal to divide the heterogeneous network architecture, consisting of multiple levels of nodes and networks, into three domains (service, logical, and physical), intra-domain hypergraphs and cross-domain hypergraphs were constructed using hypergraph theory. Further, a power heterogeneous wireless network resource slicing method based on congruence entropy is proposed, in which the underlying physical network is first divided into three virtual subnets according to the service functions in the algorithm, and then an optimization model for maximizing the node and link utilization is established according to the different demands of the three major services of the 5G network. In solving the problem, we first decouple the link conditions, which are coupled due to variables in the link mapping problem. Then, we partition them into a mapping problem between two adjacent nodes. Subsequently, we solve the node problem and link split separately using the Lagrangian pairwise decomposition method to achieve optimal deployment of the service function chain. The method is based on the simultaneous request of multiple different types of services with real-time, fast and efficient characteristics, which can meet the demand of customized service scenarios for future 5G networks. Its execution time, resource utilization, and other aspects perform better while incorporating some AI methods in the future work to align with the intelligent network operation requirements.

Acknowledgements

This study was funded by the Science and Technology Project of State Grid Corporation of China (5108-202218280A-2-415-XG).

Author contributions

WW and HZ contributed to conceptualization; CJ and HZ provided methodology; LY provided software; WW carried out formal analysis; WW performed writing—original draft; CJ performed writing—review and editing; and DZ performed supervision. All authors have read and agreed to the published version of the manuscript.

Funding

This project was supported by the Science and Technology Project of State Grid Corporation of China (5108-202218280A-2-415-XG).

Availability of data and materials

The authors confirm that the data supporting the findings of this study are available within the article.

Declarations

Competing interests

The authors declare no competing interests.

Received: 18 December 2023 Accepted: 8 March 2024

Published online: 22 March 2024

References

1. T.L. Ren, *Research on 5G Network Slicing Resource Management Algorithm for Power Communication* (North China Electric Power University, 2022)

2. Y. Gao, Z. Zhang, H. Lin, X. Zhao, S. Du, C. Zou, Hypergraph learning: methods and practices. *IEEE Trans. Pattern Anal. Mach. Intell.* **45**, 1–1 (2021)
3. X.L. Wang, *Research on Virtual Resource Management Technology for 5G Network Slicing* (Information Engineering University of the Strategic Support Force, 2019)
4. O.A. Latif, M. Amer, A. Kwasinski, Hypergraph theory for network slicing, in *2022 International Conference on Electrical and Computing Technologies and Applications (ICECTA)* (IEEE, Ras Al Khaimah, 2022), pp. 283–286
5. C. Zhuansun, K. Yan, G. Zhang, Z. Xiong, C. Huang, Hypergraph-based resource allocation for ultra-dense wireless network in industrial IoT. *IEEE Commun. Lett.* **26**(9), 2106–2110 (2022)
6. H. Zhang, L. Song, Y. Li, G.Y. Li, Hypergraph theory: applications in 5G heterogeneous ultra-dense networks. *IEEE Commun. Mag.* **55**(12), 70–76 (2017)
7. Y.H. Zang, H.K. Zheng, S.H. Yin, Resource allocation strategy for 5G network slicing oriented to new power systems. *Hebei Electr. Power Technol.* **42**(01), 26–31 (2023)
8. J. Huang, F. Yang, Y.Z. Xie, Spectrum sharing strategy for network slicing in cognitive capacity collection networks. *J. Commun.* **42**(07), 189–197 (2021)
9. J.L. Wang, Virtual network resource allocation algorithm based on genetic algorithm under network slicing. *Jiangsu Commun.* **37**(06), 22–25 (2021)
10. G.F. Zhao, *Research on Reliability-oriented 5G Network Slicing Mapping Algorithm* (Chongqing University of Posts and Telecommunications, 2020)
11. M.Y. Liu, *Research on 5G Network Slicing Resource Allocation Algorithm for Smart Grids* (North China Electric Power University, Beijing, 2022)
12. C. Song, C. Ma, Distributed multi-node slicing model and application analysis for power information collection scene, in *2022 China International Conference on Electricity Distribution (CICED), Changsha, China* (2022), pp. 1222–1227
13. Y. Zhao, J. Shen, X. Qi, X. Wang, X. Zhao, J. Yao, A 5G network slice resource orchestration and mapping method based on power service, in *2022 IEEE 6th Information Technology and Mechatronics Engineering Conference (ITOEC), Chongqing, China*, (2022), pp. 1419–1422
14. Q.Y. Sun, P. Lu, W. Lu, Forecast-assisted NFV service chain deployment based on affiliation-aware VNF placement, in *2016 IEEE Global Communications Conference (GLOBECOM)* (2016), pp. 1–6

Publisher's Note

Springer Nature remains neutral with regard to jurisdictional claims in published maps and institutional affiliations.